Pergamon
www.elsevier.com/locate/asr
Available online at www.sciencedirect.com
SCIENCE DIRECT
doi: 10.1016/S0273-1177(03)00276-X

HIGH ORDER SPECTRAL ANALYSIS OF ELECTRON PLASMA OSCILLATIONS IN THE ELECTRON FORESHOCK

S. N. Walker [1], J. S. Pickett [2], D. A. Gurnett[2], H. Alleyne[1]

[1] *ACSE, University of Sheffield, Sheffield, S1 3JD, UK*
[2] *Dept. Physics and Astronomy, University of Iowa, Iowa City, Iowa, IA 52242, USA.*

ABSTRACT

The electron foreshock is the region in which electrons that have been reflected from the shock propagate back upstream along the magnetic field lines forming electron beams. The process of relaxation of these beams is one of the fundamental topics in plasma physics. It involves numerous nonlinear processes. High order spectral analysis is applied to Cluster measurements to assess the strength of various nonlinear processes involved in the dynamics of the turbulence.

INTRODUCTION

The particle population within the electron foreshock is characterised by a population of backstreaming electrons. Observed upstream of the shock, in a region magnetically connected to it, these intermittent particle beams are responsible for the generation of intense electrostatic Langmuir waves. Nonlinear coupling of these waves with either other Langmuir waves or sound waves generate electromagnetic emissions at the plasma frequency (ω_{pe}) and its second harmonic.

The nonlinear wave-wave interactions observed in space plasma fall into one of two classes, either a three wave interaction (parametric decay instability) or a four wave interaction (modulational instability) (Kellogg et al., 1996). These instabilities possess characteristic signatures that may show up in their Fourier spectra and will be evident in their high order bi- and tri- spectra and coherence. For cases which involve Langmuir waves generated by electron beams in the foreshock, the Fourier spectrum resulting from the three wave decay instability would be characterised by two peaks in the vicinity of the plasma frequency together with a peak at a frequency equal to the difference between the two Langmuir peaks in the plasma rest frame. The Fourier spectrum resulting from a four wave modulational instability is characterised by the main emission frequency together with sidebands and a low frequency component. Often the sidebands broaden, merging with the central carrier frequency.

Emissions at the plasma frequency (ω_{pe}) may be generated by one of two mechanisms. The first involves nonlinear interactions between the Langmuir wave and low frequency ion sound waves via the decay instability. The second mechanism involves mode conversion and is dependent upon the plasma density (Yin et al. 1998; Schriver et al. 2000). Emissions at $2\omega_{pe}$ are thought to be generated by the interaction of two Langmuir waves travelling in opposite directions. The initial Langmuir waves may occur either due to the decay instability involving the initial Langmuir wave and a low frequency ion acoustic wave or by scattering caused by density irregularities.

In this paper, high order spectral techniques are used to investigate non-linear processes within the data. This paper is limited to the use of bicoherence and hence three wave interactions. The application of tri-coherence analysis to investigate four wave interactions is deferred to a later publication.

Adv. Space Res. Vol. 32, No. 3, pp. 309–314, 2003

Printed in Great Britain
0273-1177/$30.00 + 0.00

DATA

The data used in this analysis were collected by the Cluster Wideband (WBD) instrument onboard satellite 1 (Gurnett et al. 1997). Throughout the period studied the instrument was operated in the 77 kHz bandwidth mode with a base frequency of 0 kHz and a digitisation level of 8 bits. In this mode there is a 12 % duty cycle. The electric field is measured in a series of snapshots, sampled at a frequency of 219.5 kHz. Each snapshot consists of 1090 samples. Two snapshots are recorded back to back, producing 2180 continuous samples covering a period of 9.93 ms. The time between successive double snapshots is 69.5 ms. During this initial phase of operations the automatic gain was updated only once per second. This can result in a number of the more intense waveforms being clipped whilst the weaker signals clearly show the levels of digitisation used.

ANALYSIS

During the outbound leg of its orbit on 5^{th} February, 2001 the Cluster satellites made several crossings of the bow shock between 0330 and 0530 UT. The final crossing at around 0525 UT occurred at a the position (11.9, 8.8, 8.2) R_e GSE. Once through the shock the satellites entered a region in which the magnetic field lines were still connected through the shock before the field rotated at around 05:55 UT such that the satellites were no longer connected to the shock. During this traversal of the electron foreshock strong electric field wave activity in the vicinity of the local plasma frequency was observed. The intensity of these emissions peaked at around 05:53 UT just as Cluster crossed the foreshock boundary, just before entering the upstream solar wind.

The spectrogram in Figure 1 shows one second averages of the wave activity encountered as Cluster 1 approached and then crossed the electron foreshock boundary at around 05:53:47 UT. Between 05:50 and 05:53:30 UT there are strong emissions in the frequency range 20-40 kHz. As the satellite approached the boundary, the amplitude of the emissions is seen to increase until at 05:53:30 the large bandwidth emissions suddenly stop and are replaced by more discrete but intense banded emissions. In what follows, we will present the results of analysis performed on snapshots measured in this region. At around 05:53:47 UT these emissions cease as the spacecraft then enters the solar wind.

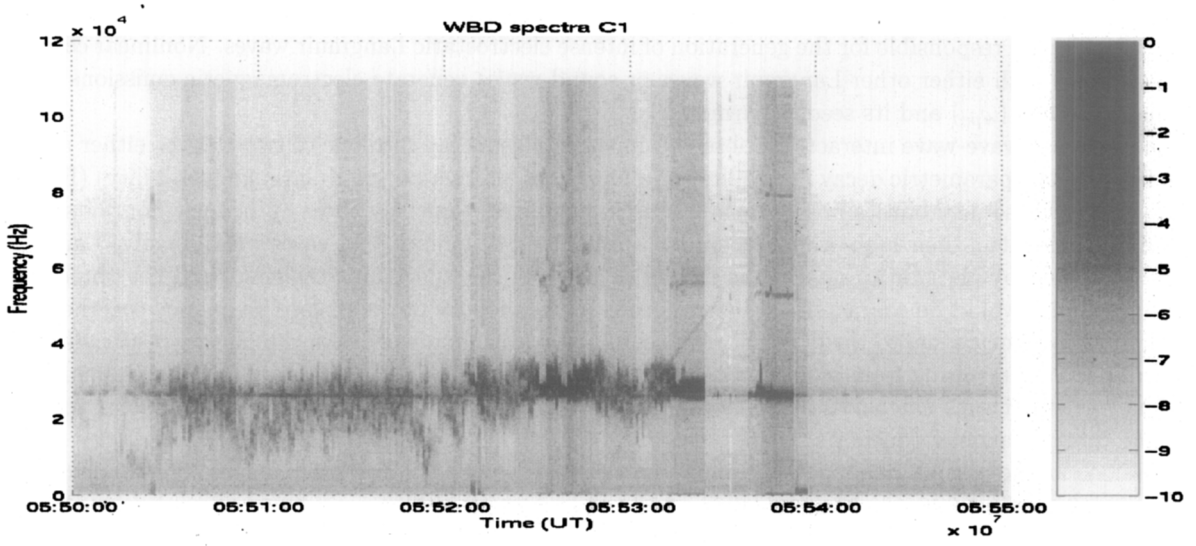

Fig. 1. Spectrogram of wave emissions measured by the WBD instrument on Cluster 1 as the satellite approached and then crossed the electron foreshock boundary.

In this paper high order spectral analysis techniques are used to find evidence for nonlinear interactions between the observed waves. Nonlinear interactions between spectral components occur if the resonance

conditions (Sagdeev and Galeev, 1969) are satisfied. For a three wave parametric decay interaction, these conditions may be expressed as $f_1 + f_2 = f_3$ and $\vec{k_1} + \vec{k_2} = \vec{k_3}$ where f_i and $\vec{k_i}$ represent the frequency and wave vector of spectral component i. Since the wave number is directly related to the phase of the wave then the phases of the three waves will also be related. The relationship between the phases of the waves involved in the interaction are investigated statistically using bispectrum and bicoherence analysis methods. The bispectrum $\mathcal{B}_f$ is defined as $\mathcal{B}_f(f_1, f_2) = \langle X(f_1)X(f_2)X^*(f_1 + f_2)\rangle$ where $X(f_i)$ represents the signal $X(t)$ filtered at frequency f_i and X^* is its complex conjugate. The bicoherence b represents the normalised bispectrum and is given by $b^2(f_1, f_2) = \frac{|\mathcal{B}_f(f_1,f_2)|^2}{\langle|X(f_1)X(f_2)X^*(f_1+f_2)|\rangle^2}$. Frequency decomposition of the signal is carried out using Fourier techniques on data intervals of 128 points. This allows the ensemble averaging to take place over 17 intervals to improve the statistics.

RESULTS

Figure 2 shows results of our analysis applied to data from the WBD instrument collected in the vicinity of electron foreshock boundary. The top panel shows the waveform of the electric field measured during one double snapshot period. A number of wave packets are observed with amplitudes in the range 0.4-0.7 mVm^{-1}. The amplitude of each packet is clearly modulated by a lower frequency. The middle panel shows the frequency spectrum of the electric field calculated using a single 2048 point FFT. The two largest peaks are observed at frequencies of 31.5 and 26.7 kHz. At lower frequencies there is a small peak corresponding to 5.2 kHz, which represents the frequency difference between the two largest peaks. Thus it appears that the decay instability was operating at this time between the Langmuir wave and the low frequency wave, generating a second Langmuir wave. There are also significant emissions frequencies lower than this. At higher frequencies there is evidence for emissions at 57.9 and 62.4 kHz. The former represents the sum of the frequencies at which the large peaks occur, the latter is the second harmonic of the higher frequency. The bottom panel shows the results of a bicoherence analysis using a 128 point FFT. It clearly shows evidence for nonlinear 3-wave interactions. There are peaks that correspond to the interactions mentioned above as well as evidence for generation of the third harmonic (i.e. $\approx 30 + \approx 60 \rightarrow \approx 90$ kHz). These harmonic frequencies are also observed to interact with the low frequency emissions observed at frequencies of 5 kHz and below. These interactions are summarised in Table 1.

An example of a possible occurrence of the modulational instability (4-wave) is shown in Figure 3. Its format is the same as that of Figure 2. The waveform shows a number of packets of electrostatic emissions whose amplitude varies in the range 0.2-0.3 mVm^{-1}. The spectra of this double snapshot is significantly different from the one described above in that it shows three closely spaced peaks at frequencies of 25.6, 28.2, and 31.2 kHz. There is also a peak at low frequencies ≈ 1.8 kHz. The results of the bicoherence analysis show only one significant peak at frequencies of ≈ 26.7 and ≈ 26.0. However, since bicoherence analysis can only be used to examine the data for three wave interactions, this result is not unexpected. A proper investigation on this snapshot requires a four wave tricoherence analysis to be performed to determine if in fact the phases of the four frequency components mentioned above are actually related. This analysis is

Table 1. The principle nonlinear interactions that exist in the dataset shown in Figure 2.

F_1	F_2	F_3	
31.5	26.5	5.2	Difference between principal peaks.
31.5	26.5	57.9	Sum of principal peaks.
31.5	31.5	62.4	2^{nd} harmonic generation.
≈ 60	≈ 30	≈ 90	3^{rd} harmonic generation.
≈ 30	≈ 5	≈ 35	Principal peaks and low frequency waves.
≈ 60	≈ 5	≈ 65	2^{nd} harmonic and low frequency waves.
≈ 90	≈ 5	≈ 95	3^{rd} harmonic and low frequency waves.

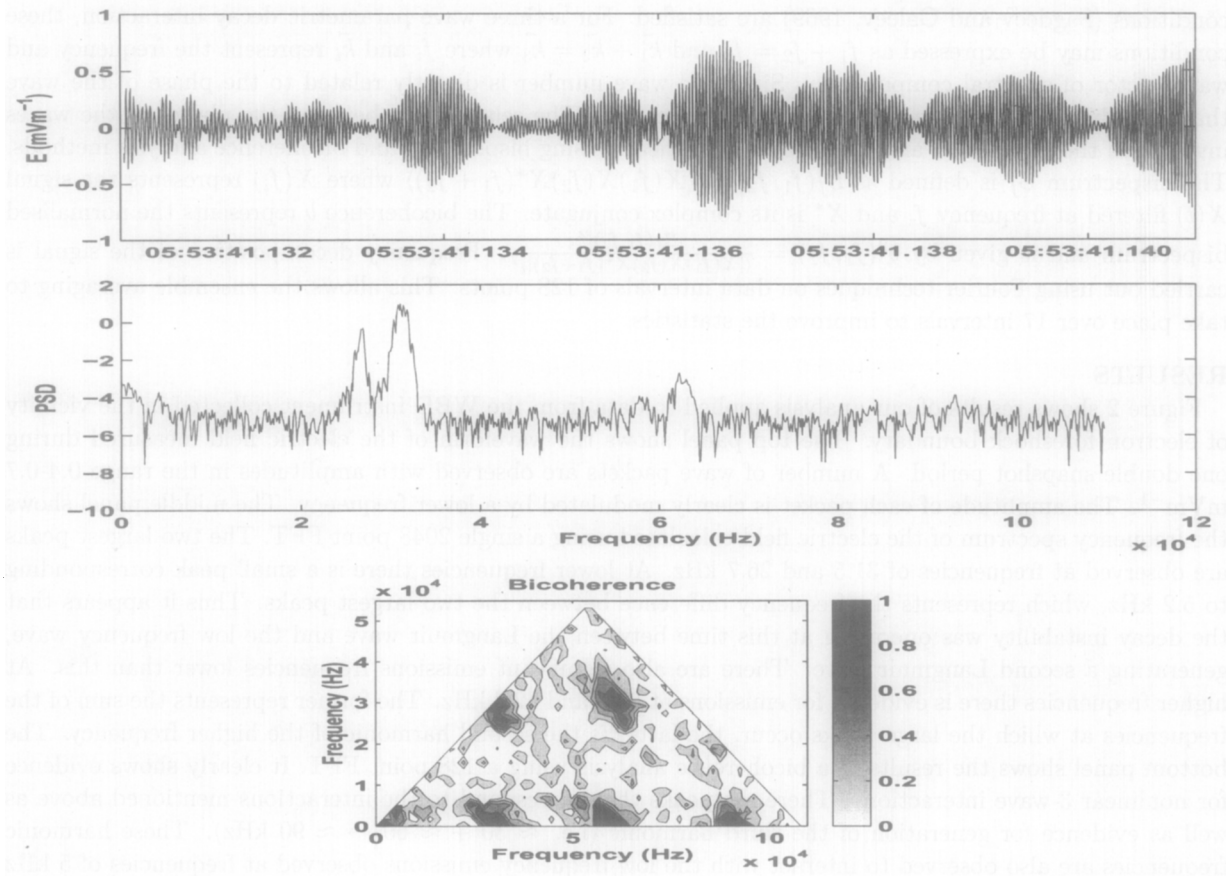

Fig. 2. The waveform (top panel), its 2048 point FFT (middle panel) and the bicoherence results (bottom panel) using a 128 point FFT.

beyond the scope of the present paper.

One question that should be addressed is that related to instrumentally generated nonlinear effects. These effects arise from the operation of the instrument and may be due to the level of digitisation employed, an inappropriate gain setting for the amplitude of emissions encountered, or the mixing of frequencies without adequate filtering of the output frequency. It was shown (Walker et al. 2002, 2000) that for test signals fed to the WBD instrument, data digitised to a level of 4 bits generated more spurious nonlinear signatures than did the use of 8 bit. Since the data analysed were collected using 8 bit digitisation and using baseband we would expect that any spurious nonlinear effect observed in the data would be produced by the instrument using an inappropriate gain setting. This would lead to either clipping of the waveform or a low amplitude waveform clearly showing levels of digitisation.

Figure 4 shows the waveform, spectrum and bicoherence results in which the waveform is clearly clipped. The spectrum of this snapshot shows that the signal contains many frequency components, the most prominent of which has a frequency of 26.7kHz. Based upon the results described in Walker et al. (2002) we would expect to see harmonics of this frequency. Examination of the spectrum shows that there are frequency components at the second (53.1 kHz) and third (79.5 kHz) harmonics present and that whilst the fundamental has the highest amplitude, the third harmonic has a higher amplitude that the second. This result would not be expected if the phenomena were natural. It is, however, expected if we analyse a square wave. Most peaks in this spectrum can be explained if it is assumed that there are two input signals of f_1=26.5 and f_2=3.9 kHz. Following Walker et al. (2002) if the two frequencies (and their harmonics) are mixed, then the components with the largest peaks occur at frequencies given by $f_1 + n * f_2$ where n is even,

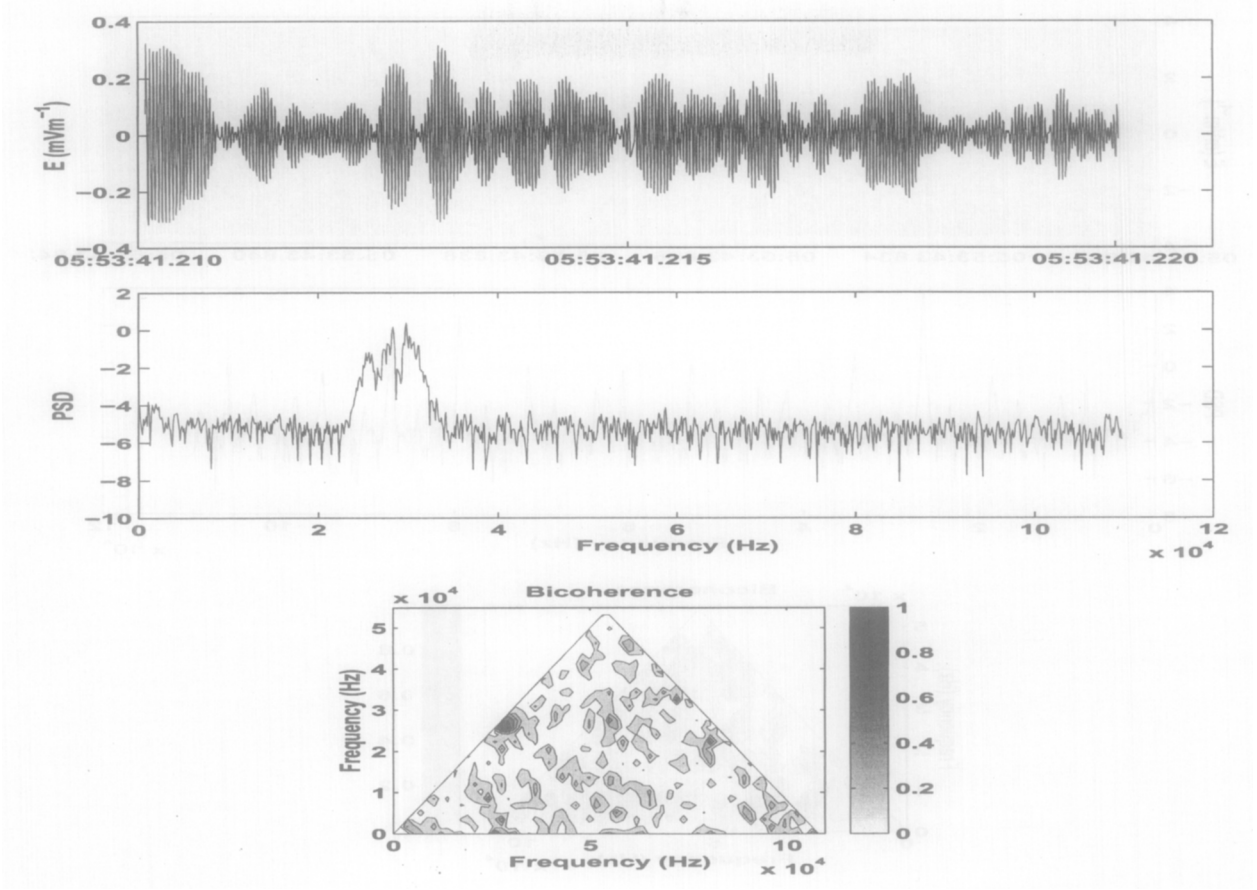

Fig. 3. Same format as Figure 2.

$2 * f_1 + n * f_2$ where n is odd, and $3f_1 + n * f_2$ where n is again even.

CONCLUSIONS

In this paper, we have shown two examples of naturally occurring nonlinear wave-wave interactions that were observed by the WBD instrument in the vicinity of the electron foreshock boundary. The spectra of these two events showed the typical characteristics expected for the occurrence of the parametric decay and modulational instabilities. Thus these mechanisms play a role in the evolution of the Langmuir waves, generated by beams of electrons reflected at the terrestrial bow shock, to produce the turbulent spectrum observed in the electron foreshock region. These processes provide one particular path by which energy from the incoming solar wind is redistributed at the terrestrial bow shock and dissipated within the foreshock region. An analysis was also carried out on a clipped waveform snapshot. It was shown that it contained a pattern of peaks that is characteristic of a square wave.

ACKNOWLEDGEMENTS

SNW wishes to thank PPARC for financial support through grant PPA/G/R/1999/00487. JSP and DAG acknowledge support from NASA/GSFC under Grant NAG5-9974.

REFERENCES

Bale, S. D., D. E. Larson, R. P. Lin, et al., On the beam speed and wavenumber of intense electron plasma waves near the foreshock edge, *J. Geophys. Res. A* **105**, 27353, 2000.

Fitzenreiter, R. J., The electron foreshock, *Advances in Space Research* **15**, 9, 1995.

Gurnett, D. A., R. L. Huff and D. L. Kirchner, The wide-band plasma wave investigation, *Sp. Sci. Rev.*

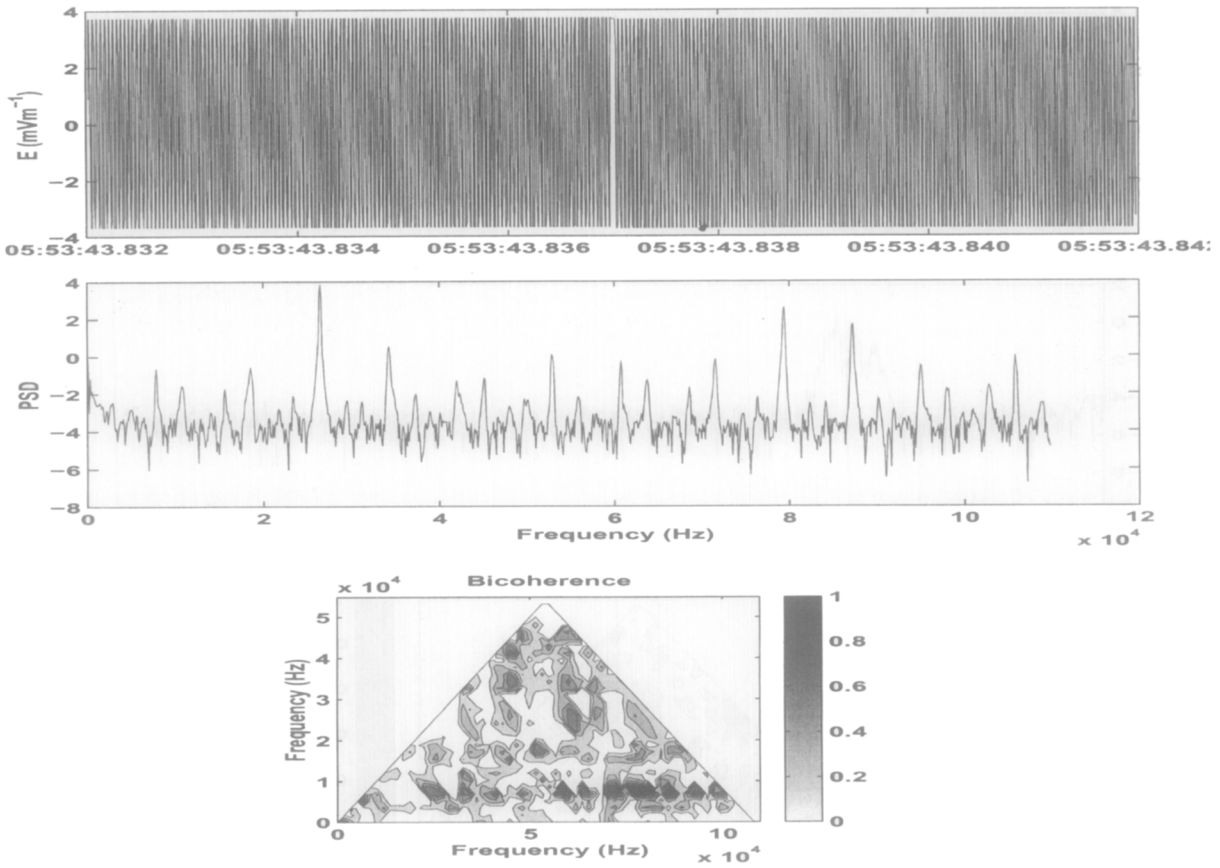

Fig. 4. Same format as Figure 2. In this case the wave form snapshot is clipped.

79, 195, 1997.

Kellogg, Paul J., Steven J. Monson, Keith Goetz, et al., Early wind observations of bow shock and foreshock waves, *Geophys. Res. Lett.* **23**, 1243, 1996.

Sagdeev, R. Z., and A. A. Galeev, *Nonlinear Plasma Theory*, p.6 Benjamin, White Plains, N.Y., 1969.

Schriver, D., M. Ashour-Abdalla, V. Sotnikov, et al., Excitation of electron acoustic waves near the electron plasma frequency and at twice the plasma frequency, *J. Geophys. Res. A* **105**, 12919, 2000.

Walker, S. N., R. Huff, and M. A. Balikhin, An investigation into instrumental nonlinear effects, *Proc. Cluster II workshop on multiscale/multipoint measurements*, ESA-SP449, p.279, 2000.

Walker, S. N., M. A. Balikhin, I. Bates, and R. Huff, An investigation into instrumental nonlinear effects, in press, Advances in Space Research, 2002.

Yin, Y., M. Ashour-Abdalla, M. El-Alaoui, et al., Generation of electromagnetic f_{pe} and $2f_{pe}$ waves in the Earth's electron foreshock via linear mode conversion, *Geophys. Res. Lett.* **25**, 2609, 1998.

Corresponding author: simon.walker@shef.ac.uk

Manuscript received 26th November 2002; revised 24th February; accepted 7th March, 2003